Journal of Imaging Science and Technology® 57(3): 030402-1–030402-7, 2013.

Three Dimensional Simulation of Toner Scattering with an Intermediate Transfer Belt

Masami Kadonaga
Digital Engineering Center, RICOH Company, LTD, 810, Shimo-Imaizumi, Ebina-Shi, Kanagawa 243-040, Japan
E-mail: masami.kadonaga@nts.ricoh.co.jp

Abstract. *A three dimensional calculation of a first transfer subsystem in electrophotography is carried out and toner scattering on a transfer belt is simulated. This simulation consists of an electric field calculation and a toner movement calculation, and toner scattering around the periphery of the dot is investigated. The simulation shows that the formation of toner scattering arises from the toner jumping across the transfer gap before the photoconductor contacts the belt. The effects of transfer parameters on toner scattering are investigated with the simulation. To prevent toner scattering, the position of the roller, adhesion force, transfer bias, toner charge, and resistivity of the belt should be optimized to create an appropriate electric field distribution, and so that the toner transfer occurs in a small gap or in a contact nip between the photoconductor and the belt. © 2013 Society for Imaging Science and Technology.*
[DOI: 10.2352/J.ImagingSci.Technol.2013.57.3.030402]

INTRODUCTION

Intermediate transfer belt systems have been widely used in electrophotography. The system includes two transfer processes (a first and a second transfer), as shown in Figure 1. A toner image developed on a photoconductor is primarily transferred onto an intermediate transfer member in the first transfer process, and is then secondarily transferred onto a sheet of paper in the second transfer process. Since toner images are transferred by electrostatic force, the design of their electric field distribution is a key point for faithful transfer, and the system realizes high image quality when the transfer conditions are properly optimized. Image degradation in the transfer processes, such as toner scattering (satellites), halo, hollow character, and mottle, is a serious problem in obtaining a faithful transfer. The degradation is not readily examined using a real electrophotography machine because it is difficult to precisely determine under what specific conditions transfer occurs. It is useful to investigate transfer phenomena with a numerical simulation under well-defined conditions, and some interesting studies have been reported.[1,2] To investigate alphanumeric images and halftone dots, two dimensional analysis is not appropriate, because it cannot reproduce such images. In this study, a three dimensional simulation for a first transfer process is developed to investigate toner scattering with such images. An example of toner scattering around a 2 × 2 dot image is presented in Figure 2. One can easily imagine that such toner scattering would adversely affect image quality such as resolution and granularity. This is one of the persistent problems in the development of transfer systems, and many hypotheses on toner scattering have been presented in previous works.[3–5] Toner particles are highly charged and they are mutually repulsive. This repulsive electrostatic force between toner particles can cause the particles to fly apart and generate scattered images. This article will discuss toner scattering due to the repulsive force while the toner particles are flying from the photoconductor to the transfer belt.

Received Dec. 13, 2012; accepted for publication Apr. 22, 2013; published online May 1, 2013. Associate Editor: Michael Lee.
1062-3701/2013/57(3)/030402/7/$20.00

SIMULATION MODEL

A schematic diagram of a first transfer process is presented in Figure 3. It consists of an organic photoconductor, a transfer belt, and a transfer roller. In the initial state, a latent image and toner particles are deposited on the surface of the photoconductor, and toner particles adhere to the photoconductor because of an adhesion force, which includes electrostatic and Van der Waals forces. Figure 4 shows the simulation area of the first transfer process, which includes a photoconductor, a latent image, toner particles, a belt, and a transfer roller. Figure 5 shows a magnified view of the calculation mesh around the toner particles deposited on the photoconductor. The size of calculation mesh is almost as large as that of the toner particle.

From our previous study, toner scattering occurs in a pre-nip region of the first transfer area due to the repulsive force between toner particles.[6] Therefore the electric field and the motion of the toner particles should be calculated simultaneously because the movement of toner alters the electric field distribution around it. The electric field $\boldsymbol{E}$ and the electric potential ϕ in the analysis area are obtained with the Poisson equation:

$$div(\varepsilon \cdot \boldsymbol{E}) = -div(\varepsilon \cdot grad\phi) = \rho, \tag{1}$$

where ρ is the electric charge density and ε is the permittivity. The electric charge density ρ is calculated by considering transport of electric charges and electrostatic discharge. The transport of the electric charges is expressed by the equation of continuity:

$$\frac{\partial \rho}{\partial t} = -div\,\boldsymbol{J}, \tag{2}$$

where t is the time and $\boldsymbol{J}$ is the current density.

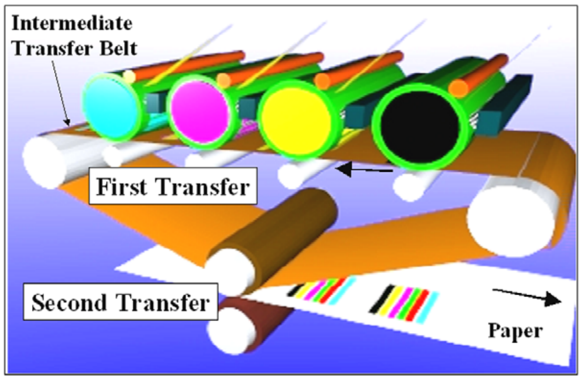

Figure 1. The intermediate transfer belt system includes two transfer processes: a first and a second transfer.

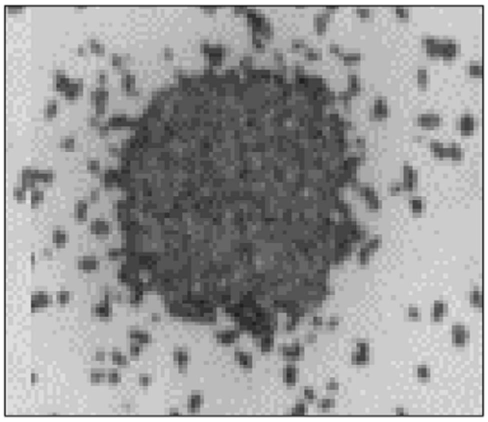

Figure 2. Toner scattering around a 2 × 2 dot image. Toner particles cluster around the original image and the dot is badly disrupted.

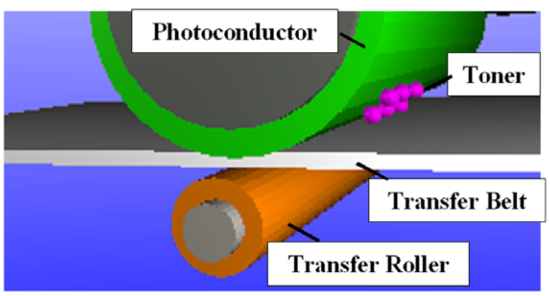

Figure 3. A first transfer process that consists of a photoconductor, a transfer belt and a transfer roller.

The current density $\boldsymbol{J}$ is calculated including the electrical conduction and the convection as follows:

$$\boldsymbol{J} = \sigma \cdot \boldsymbol{E} + \rho \cdot \boldsymbol{v}_p, \tag{3}$$

where σ is the electrical conductivity and $\mathbf{v}_p$ is the process velocity of the transfer system.

Electrostatic discharges occur in some air gaps (between the photoconductor and the belt, and between the belt and the roller). The effect of the discharges is considered by adding electric charges on the object surfaces forming an air gap, when the electric potential difference across the air gap

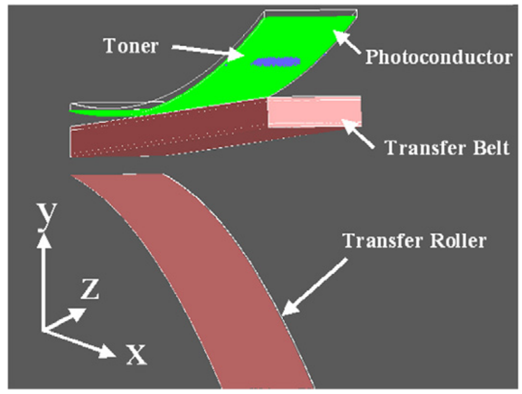

Figure 4. The simulation area of the first transfer process, which includes a photoconductor, a latent image, toner particles, a belt, and a transfer roller.

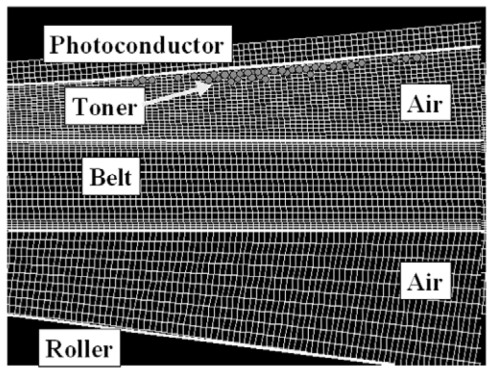

Figure 5. Magnified view of the calculation mesh around toner. The size of the calculation mesh is almost as large as that of the toner particle.

exceeds the Paschen limit. The relations between the Paschen limit ϕ_{pa} and the air gap G [m] are as follows:[7]

$$\phi_{pa} = \begin{cases} 75.4 \times 10^6 \cdot G & (G < 4.8 \times 10^{-6}) \\ 362 & (8.0 \times 10^{-6} \geq G \geq 4.8 \times 10^{-6}) \\ 312 + 6.2 \times 10^6 \cdot G & (G > 8.0 \times 10^{-6}). \end{cases} \tag{4}$$

The amount of electrostatic discharge Q [C/m^2] is estimated by the following equation:

$$Q = \varepsilon_0 \cdot (\Delta\phi - \phi_{\mathrm{pa}}) \frac{\sum\left(\frac{d_i}{\varepsilon_i}\right) + G}{G \cdot \sum\left(\frac{d_i}{\varepsilon_i}\right)}, \tag{5}$$

where $\Delta\phi$ is the electric potential difference across the air gap, ε_o is the vacuum permittivity, and ε_i and d_i are the relative dielectric constant and the thickness of objects, respectively.[7]

The electrostatic force acting on a toner particle $\boldsymbol{F}_e$ is related to the quantity of electric charge of the toner particle q and the electric field $\boldsymbol{E}$ as follows:

$$\boldsymbol{F}_e = q_i \cdot \boldsymbol{E} + \sum_{j=1(i \neq j)}^{N} \frac{q_i \cdot q_j}{4\pi\varepsilon_0 L^2}, \tag{6}$$

where L is the distance between toner-i and toner-j, N is the total number of toner particles, and q_i is the charge of toner-i. The repulsive forces between toner particles are superimposed in Eq. (6), because the size of the calculation mesh is not small enough to estimate the electric field strictly. (The size of the toner particles is 6 μm and the size of the mesh is about 5 μm.)

The motion of the toner is calculated by Newton's second law of motion:

$$\boldsymbol{F}_e = \frac{\mathrm{d}\,(m_t \cdot \boldsymbol{v}_t)}{\mathrm{d}t}, \tag{7}$$

where m_t and $\mathbf{v}_t$ are the mass and the velocity of the toner, respectively. In the present model, the toner begins to move when the electrostatic force acting on the toner overcomes the adhesion force, and continues to move until it reaches the surface of the belt. It is well known that the value of the electrostatic adhesion force is greater than that of the theoretical one. Although $\boldsymbol{F}_e$, obtained from Eq. (6), includes electrostatic forces theoretically, the adhesion force, which is used to decide toner flying, includes non-electrostatic and electrostatic forces. The value of the adhesion force is determined from measurements. Collisions and adhesion forces between toner particles would not play an important role for toner scattering once they fly apart from the photoconductor. Those effects are not considered in this simulation.

The electric field $\boldsymbol{E}$ and the electric potential ϕ are solved again by the Poisson equation (Eq. (1)) because the electrical conduction, the advection, the discharges and the movement of toner particles alter the electric field distribution. These steps are repeated until all the toner particles are transferred to the belt.

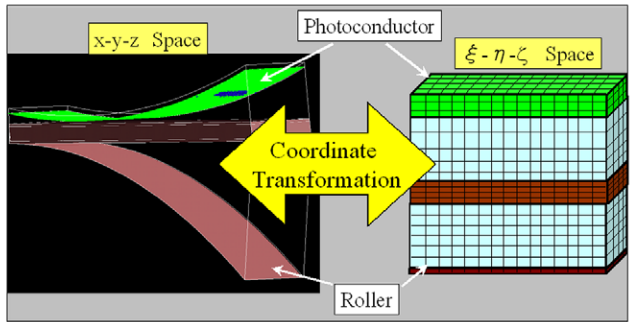

Figure 6. Schematic diagram of the transformation form x–y–z space to ξ–η–ζ space.

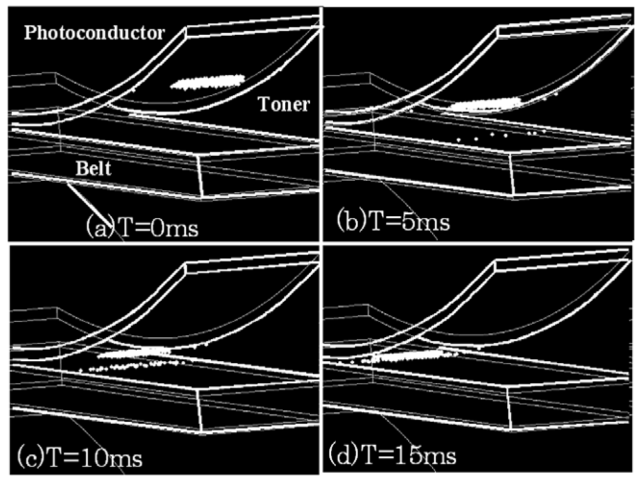

Figure 7. Sequence of the simulation results, which demonstrate the movement of toner particles. At $T = 5$ ms, some toner particles are transferred, and at $T = 15$ ms, all the toner particles are transferred to the belt.

SIMULATION RESULT

The simulation is carried out with a boundary fitted coordinate system (BFC). With the system, the Cartesian coordinates (x, y, z) are transformed into the boundary fitted coordinates (ξ, η, ζ), as is shown in Figure 6. Thanks to this transformation, finite difference methods can readily be used to solve the equations mentioned above. The method is popular in the field of fluid dynamics simulation, and two dimensional analyses with the system are already applied in simulations of charging and transfer processes of electrophotography.[2,8]

Figure 7 shows the sequence of the simulation results, which demonstrate the movement of toner particles. The diameter of the toner particles is 6 μm and the adhesion force is 70 nN, which is the sum of electrostatic and Van der Waals forces between toner and photoconductor. On the photoconductor, a 2 × 2 dot latent image and 480 toner particles are deposited, and transfer bias (600 V) is applied on the transfer roller. At $T = 5$ ms, some toner particles are transferred, and at $T = 15$ ms, all the toner particles are transferred to the belt. Figure 8 shows the top view of the toner particles transferred to the belt; except for Fig. 8(a), which indicates a dot image on the photoconductor before transfer. The dot before transfer is well formed, and it exhibits minimal satellite formation. However, it is found that after transfer, the dot is disrupted. Comparison between Fig. 8(a) and (d) shows that toner scattering and image degradation are easily recognized.

PARALLEL COMPUTATION

Three dimensional calculation needs an enormous number of calculation meshes. Furthermore, consideration of discharge, resistivity, convection and toner movement with the BFC system makes the simulation complicated. The simulation is so large and complex that it is impractical to solve it on a single computer with limited computer memory because it needs a considerable computational load. In order to reduce the load, the calculation is carried on the large-scale supercomputer TSUBAME at Tokyo Institute of Technology[9] and hybridization of parallel computation techniques, using Multi Processing (OpenMP) in conjunction with the Message Passing Interface (MPI), is adopted. The simulation program starts with MPI initialization and creates OpenMP parallel regions within each MPI process. Figure 9 shows the relation between calculation efficiency and the number of

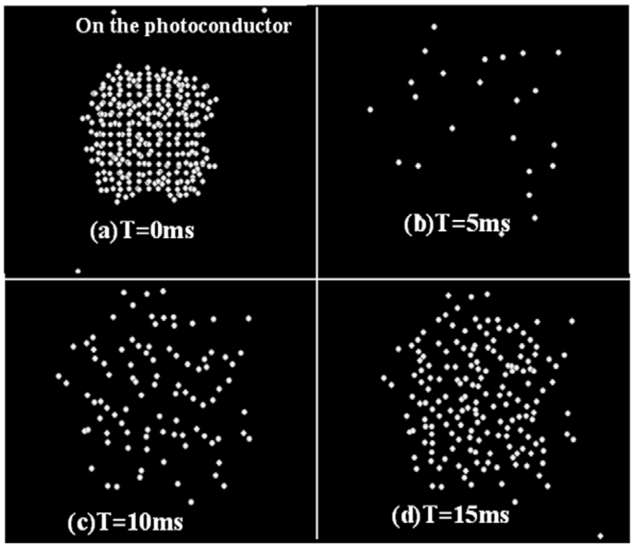

Figure 8. Top view of the toner particles transferred to the belt, except for (a), which indicates the toner image on the photoconductor before transfer.

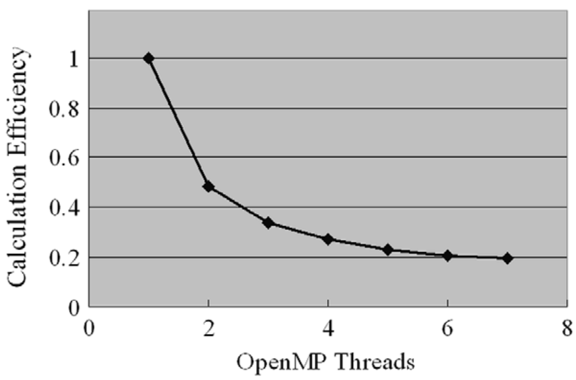

Figure 9. Relation between the calculation efficiency and the number of threads for OpenMP without MPI.

threads for OpenMP without MPI. The calculation efficiency is the ratio defined as follows:

Calculation efficiency = (calculation time with parallel computation) /(calculation time without parallel computation).

As the number of threads for OpenMP increases, calculation time reduces, but more effective reduction is needed for the 3D calculation. Figure 10 shows the relation between the calculation efficiency and the number of cores with MPI and OpenMP. The numbers (a, b, c) indicate the number of divisions for the ξ, η, ζ directions of the BFC system, respectively, and the total number of tasks is a*b*c. Division in the ξ or η direction offers good calculation efficiency. On the other hand, division in the ζ direction deteriorates the efficiency. This is probably due to a memory contention because MPI is a shared memory method. Memory allocation of the ζ direction is probably not suitable for MPI. Figure 11 shows the comparison between the calculation efficiency without MPI and that with the best configuration of MPI. The best configuration of MPI is (4, 3, 1), and the best performance is realized with

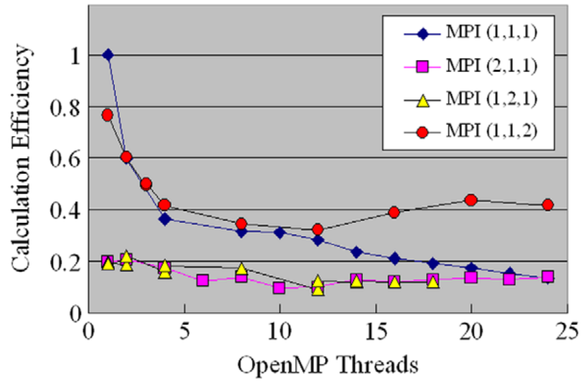

Figure 10. Relation between the calculation efficiency and the number of threads with MPI/OpenMP. The numbers (a, b, c) indicate the number of divisions for the (ξ, η, ζ) directions, respectively.

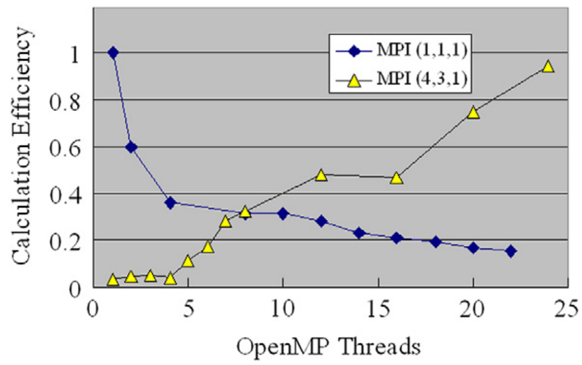

Figure 11. Comparison between the calculation efficiency without MPI and that with the best configuration of MPI.

MPI:(4, 3, 1) and OpenMP:4 threads. About 20 times faster calculation than that without a parallel technique is realized. With more than 4 threads for OpenMP with (4, 3, 1) for MPI, calculation performance becomes worse and this is probably due to the memory contention. All the calculations shown in the following sections are carried out with MPI:4*3*1-tasks and OpenMP:4 threads.

PARAMETER STUDY

The simulation can be used to investigate the mechanism of toner scattering and to optimize the parameters of the first transfer to prevent image degradation. The effect of adhesion and the position of the transfer roller, transfer bias, and toner charge are investigated and will be discussed in the following sections.

Adhesion and the position of the roller

The adhesion force between the toner and the photoconductor plays an important role in the transfer process, and is known to be a very important parameter to prevent toner scattering. The position of the transfer roller changes the electric field and also affects the image quality. The position of the roller is expressed as the offset distance between the center of the transfer roller and that of the photoconductor. A simulation condition "+2 mm" means that the roller is set in the upstream position and the distance is 2 mm.

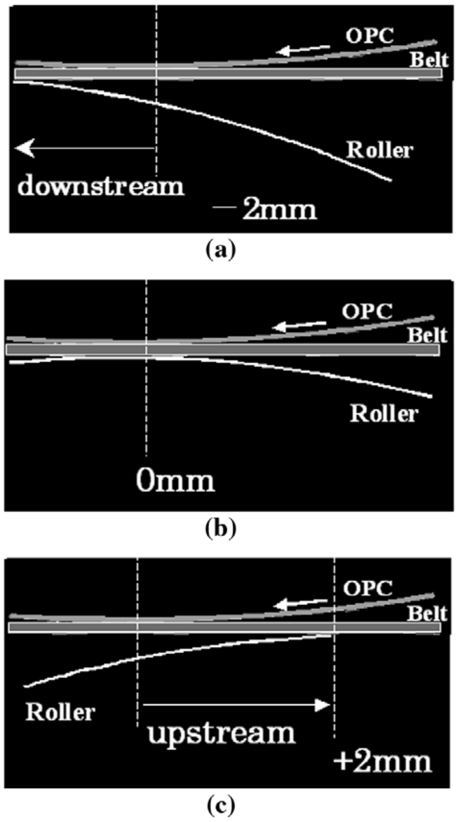

Figure 12. Position of the transfer roller. The position of the roller is expressed as the offset distance between the center of the transfer roller and that of the photoconductor.

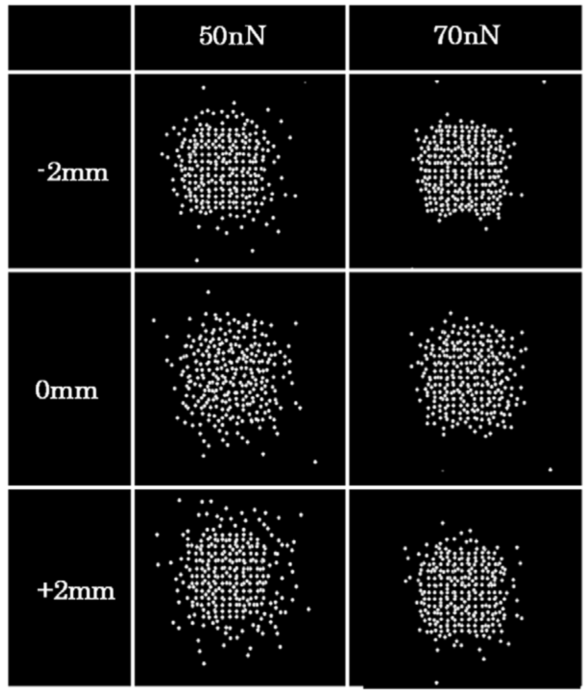

Figure 13. Simulation results with various adhesion forces and roller positions. A faithful transfer is accomplished by arranging the transfer roller in the downstream region with appropriate toner adhesion.

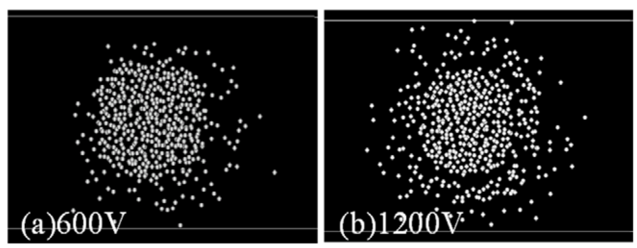

Figure 14. Image on the belt with transfer biases of 600 and 1200 V. The number of scattering toner particles increases with increasing transfer bias.

On the other hand, "−2 mm" indicates that the roller is set in the downstream position, as is shown in Figure 12. Fig. 12(a), (b), and (c) show the cases "−2 mm", "0 mm", and "+2 mm", respectively.

Figure 13 shows the simulation results for various adhesion forces and roller positions. The image with the toner adhesion of 50 nN shows a lot of scattering toner particles. This result indicates that the surface treated toner with additives which reduce adhesion increases the amount of toner scattering, because the surface treated toner is able to move across the air gap in a pre-nip region. This tendency is investigated and reported in Ref. 4.

With regard to the position of the transfer roller, the dot image after transfer is badly disrupted by arranging it in the upstream region, and this tendency can be observed in actual printers.[5] This is because if the transfer roller is arranged in the upstream region, the potential difference between the photoconductor and the transfer belt becomes large and toner particles begin to move in a pre-nip area. These results suggest that a faithful transfer is accomplished by arranging the transfer roller in the downstream region with appropriate toner adhesion.

Transfer bias

Figure 14 shows the calculated images on the belt for transfer biases of 600 and 1200 V. As the transfer bias increases, the number of scattering toner particles increases and image degradation becomes worse. This tendency is well known from many experiments.[6]

Toner charge

Figure 15 shows the results for toner charges of −20, −40, and −60 μC/g. It is found that the dots are disrupted and the number of scattering toner particles increases monotonically with increasing toner charge. This tendency is also well known from many experiments.

Belt resistivity

It is well established that the resistivity of the transfer media (belt and paper) affects image quality after transfer. The effect of the resistivity of the first transfer belt is investigated and is shown in Figure 16. Fig. 16(a), (b), and (c) show the results with an insulator belt ($\infty\Omega$ m), a belt of 10^5 Ω m, and one of 10^4 Ω m, respectively. Lower resistivity causes more image degradation and this tendency is also well known from many experiments.[5]

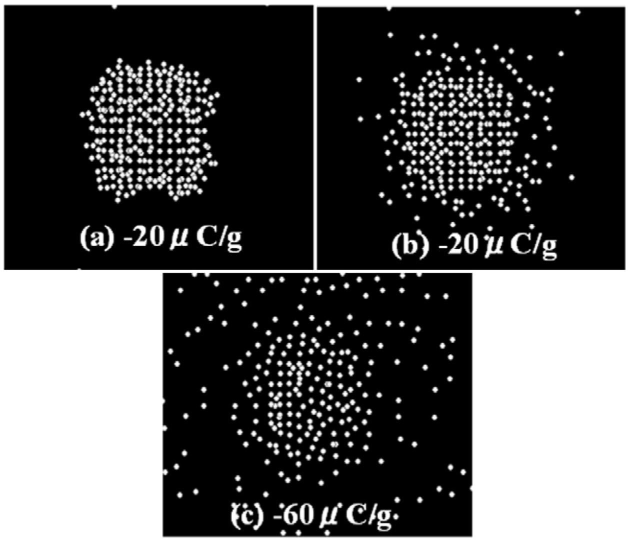

Figure 15. Image on the belt with toner charges of −20, −40, and −60 μC/g. The dots are disrupted and the number of scattering toner particles increases with increasing toner charge.

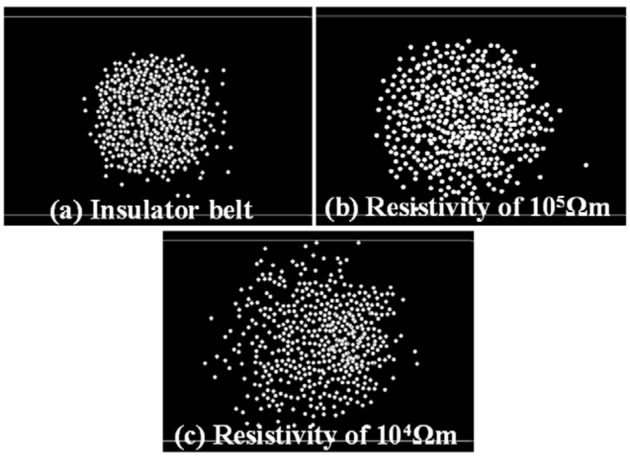

Figure 16. Dot image on an insulator belt, one with a resistivity of 10^5, and one with 10^4 Ω m. Lower resistivity causes more image degradation.

CONSIDERATION

Figure 17 shows a comparison of some typical results, and Table I shows the values of the parameters of the calculations for Fig. 17. The result of Fig. 17(a) is the worst case, and Fig. 17(d) is the best case. The toner scattering focused on in this article is due to the Coulomb force between toner particles while they are flying from the photoconductor to the transfer belt. Therefore, the transfer gap, in which toner starts to transfer, is an appropriate value to investigate the mechanism of toner scattering. Figure 18 shows a comparison of the transfer gaps between the best and the worst cases. When toner particles begin to move in a small gap, toner scattering rarely occurs, and the dot image after transfer will be fine. On the other hand, when toner particles begin to move in a large gap, the toner scattering will be enormous, and the dot image will be deteriorated. The result shows that the parameters should be optimized to create an appropriate electric field distribution and to realize toner transfer in a small gap or in a contact nip between the photoconductor and the belt.

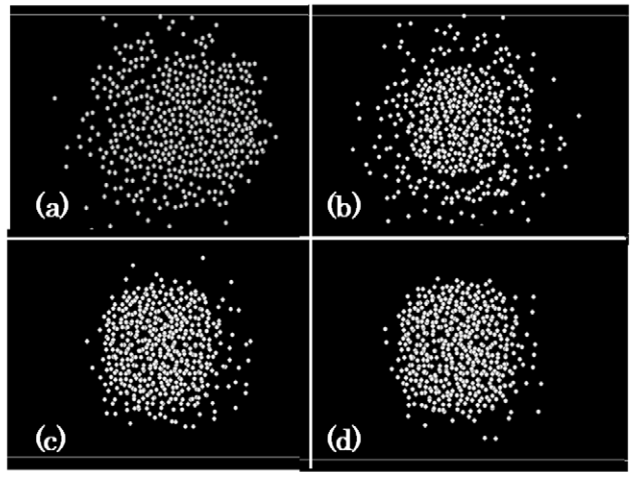

Figure 17. Comparison of some typical results with the parameters listed in Table I; (a) is the worst case and (d) is the best one.

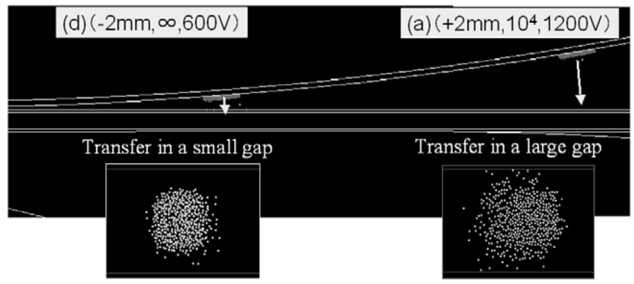

Figure 18. Comparison of transfer gaps between the best and the worst cases. The left arrow indicates a transfer gap for case (d) and the right arrow indicates a transfer gap for case (a). A smaller transfer gap leads to a fine dot image on the belt.

Table I. The values of the parameters for Fig. 17.

	Position of the roller (mm)	Resistivity of the belt	Transfer bias (V)
(a)	+2	104 Ωm	1200
(b)	+2	Insulator (?Ωm)	1200
(c)	−2	Insulator (?Ωm)	1200
(d)	−2	Insulator (?Ωm)	600

CONCLUSION

A three dimensional simulation of a transfer process is developed and carried out on the supercomputer TSUBAME, and toner scattering is simulated. The simulation consists of an electric field calculation and a toner movement calculation. The parallel calculation methods of OpenMP and MPI are used to reduce calculation time. In order to calculate the electric field precisely, a boundary fitted coordinate system is adopted, and to estimate the force on the toner in detail, the force from the electric field, the discharge phenomenon, and the toner adhesion force are considered. Toner separates from the photoconductor and begins to move downward when the electrostatic force is greater than the adhesion force, and toner movement is calculated according to Newton's law of motion. The effects of the position of the transfer roller, adhesion force, transfer voltage, and resistivity of the transfer belt are investigated with the simulation and the results suggest the optimal conditions to prevent toner scattering. To suppress toner scattering, the parameters for the transfer should be optimized to create an appropriate electric field distribution and to ensure that the toner transfer occurs in a small gap or in a contact nip with the photoconductor and the belt.

FUTURE WORK

The simulation needs more realistic models to compare with experiments. Toner charge and diameter distributions, a distribution of adhesion force, a wider calculation area, collisions between toners, and the electric field dependence of the conductivity should be considered to reproduce various images on a transfer medium obtained from experiments. In the near future, with the advance of parallel calculation techniques, a more reliable 3D simulation will be established and simulation results will be compared with experiments for verification. The author hopes that 3D simulation will become a useful tool for the design and optimization of electrophotography products in the manufacturing process.

REFERENCES

[1] T. Sasaki, T. Onishi, A. Sugiyama, and S. Nasu, "Transfer process multiphysics simulation in electrophotography," J. Imaging Sci. Technol. **54**, 030505 (2010).

[2] S. Aoki, M. Sukesako, and M. Kadonaga, "Numerical simulation of toner transfer considering voltage distribution on the transfer belt," J. Imaging Sci. Technol. **52**, 051001 (2008).

[3] A. J. Rushing, R. D. Fields, D. S. Rimai, and A. Hoskins, "Toner satellite formation in electrostatically transferred images," J. Imaging Sci. Technol. **45**, 187–197 (2001).

[4] B. Gady, D. J. Quesnel, D. S. Rimai, S. Leon, and P. Alexandrovich, "Effects of silica additive concentration on toner adhesion, cohesion, transfer, and image quality," J. Imaging Sci. Technol. **43**, 288–294 (1999).

[5] H. Katayanagi, Y. Miyasaka, S. Nishida, and H. Miho, "The superior color performance of the konica minolta 8050 high-speed multifunctional peripherals (MFP)," Konica Minolta Technol. Report **1**, 67–70 (2004) (In Japanese).

[6] H. Iimura and M. Kadonaga, "An observation of toner scattering behavior in the transfer process", *Proc. IS&T's NIP24: Int'l Conf. on Digital Printing Technol. and Digital Fabrication* (IS&T, Springfield, VA, 2008), pp. 338–341.

[7] R. M. Schaffert, *Electrography* (Focal Press, London, 1975), p. 522.

[8] M. Kadonaga, T. Katoh, and T. Takahashi, "A study of non-uniform charging by charging roller with DC voltage," J. Imaging Sci. Technol. **43**, 274–279 (1999).

[9] Tokyo Institute of Technology Global Scientific Information and Computing Center web site, www.gsic.titech.ac.jp/en, accessed March 2013.